Çanakkale Onsekiz Mart University

Journal of Advanced Research in Natural and Applied Sciences

dergipark.org.tr/tr/pub/jarnas

Open Access

CC BY NC

e-ISSN: 2757-5195 | 2024, Vol. 10, Issue 3, Pages: 747-760 | doi.org/10.28979/jarnas.1481067

An Overview of Traditional and Next-Generation Earthquake Early Warning Systems

Süleyman Tunç[1], Berna Tunç[2], Deniz Çaka[3], Emrah Budakoğlu[4]

[1]Sentez Earth and Structure Engineering Limited, Dragos Park Plaza, İstanbul, Türkiye
[2,3]Department of Geophysical Engineering, Faculty of Engineering, Kocaeli University, Kocaeli, Türkiye
[4]Department of Geophysical Engineering, Faculty of Engineering, Sakarya University, Sakarya, Türkiye

Article Info
Received: 09 May 2024
Accepted: 20 Sep 2024
Published: 30 Sep 2024
Research Article

Abstract − The Earthquake Early Warning System generates rapid and effective warnings after detecting an earthquake, before the arrival of destructive waves to the areas that may be affected. In this way, it is aimed to minimize the loss of life and property. In this study, traditional early warning systems that are frequently used in the world are discussed. The details of the next-generation early warning system, which has recently produced successful outputs, are discussed, and its advantages over traditional early warning systems are mentioned. The recent developments of this system are also analyzed. Next-generation early warning systems consist of a new array-based algorithm composed of two modules for real-time epicenter detection. The detection of an earthquake occurring in the Marmara Sea (Türkiye) with a next-generation early warning system using array-based location methodology is given as an example. Next-generation early warning systems have advantages over traditional ones, such as lower cost and time gains of up to minutes.

Keywords − *Early warning systems, algorithms, seismometer, traditional, next-generation*

1. Introduction

An earthquake early warning system (EEWS) is a system that aims to send timely warnings to people or organizations at the onset of a destructive earthquake. EEWS detects the onset of an earthquake by measuring the velocity of seismic waves generated by the earthquake. EEWS requires seismic stations installed close to the source to detect earthquakes. When the destructive earthquake starts, P waves are detected by these seismic stations. Since P waves are the first to reach the stations, magnitude scaling is estimated using these waves. The system then rapidly generates a warning message, and an earthquake warning is transmitted to the public or organizations through appropriate channels (Figure 1). EEWS enables many important measures to be taken, such as opening exit doors in buildings, safely stopping escalators and lifts, stopping or controlling slowing down the activities of facilities such as factories, nuclear power plants, etc., stopping or slowing down rail systems such as high-speed trains, subways, trams, stopping microsurgical operations in hospitals. In addition, if a satisfactory warning time can be achieved, major benefits include protecting human life and reducing structural damage [1].

A frequently confused point that should be emphasized is that earthquake early warning systems cannot predict the earthquake in advance. In other words, they cannot produce a warning without detecting an earthquake. The main countries currently using EEWS in various parts of the world are India, Israel, Greece, Italy, Italy,

[1]stunc@syy.com.tr; [2]berna@kocaeli.edu.tr; [3]caka@kocaeli.edu.tr; [4]ebudakoglu@sakarya.edu.tr (Corresponding Author)

Romania, Türkiye, Taiwan, Japan, Canada, the United States of America, and Mexico [2-11]. Türkiye already has an active EEWS. However, it does not yet provide an alert to the public.

Figure 1. Overview of Earthquake Early Warning System

In EEWS, the two basic body waves, P and S waves, are of great importance. P waves are the fastest propagating seismic waves at the beginning of an earthquake. During an earthquake, P waves first vibrate the earth's crust and are used to quickly detect the onset of an earthquake. Detection and analysis of P waves allow the EEWS to determine the onset of the earthquake. S waves are the second seismic waves propagating after P waves during an earthquake. They propagate more slowly than P waves but have a greater energy. All earthquake early warning systems used worldwide are based on P-wave magnitude estimation. This is because the P wave propagates faster than the destructive S wave (generally Vp=6.0 km/s - Vs=3.5 km/s) and is the first wave to reach the stations.

For a settlement 100 km away; tp=100/6.0 = 16.7 s, ts=100/3.5 = 28.6 s. In this context, the warning time is 28.6-16.7=11.9 s (the time taken for data transmission and the processing time are set to zero; in practice, these delays and processing time should also be considered). Latency is the time it takes inside the sensor until the P-wave arrives and is packaged and placed on the transmission path. Delay refers to the time it takes for this packet to arrive at the center along the transmission line.

2. Traditional and Next Generation Earthquake Early Warning Systems

Some early earthquake early earning systems (EEWs) have been developed worldwide to estimate real-time location, magnitude, and maximum ground shaking about seismic events [12]. EEWs have two basic approaches: the single station ("on-site") approach and the network (regional) approach [13]. The in-situ EEW approach is based on the principle of detection of the P wave by a single sensor and warning before the more destructive S wave arrives. In the network approach, data from many seismic sensors are used in areas where earthquakes are likely to occur. In this approach, since multiple stations are expected to detect the earthquake, it can operate slower than the single-station approach. However, it has the advantage of fewer erroneous results. This section will briefly mention the widely used traditional and next-generation systems.

2.1. Earthquake Point-Source Integrated Code (EPIC/Elarms)

Earthquake Point-Source Integrated Code (EPIC) or Earthquake Alarm Systems (ElarmS) is a system that can provide a warning when an earthquake occurs. EPIC detects the first earthquake wave by the station closest to the fault and estimates the peak ground shaking with the information it receives [14]. The ElarmS methodology determines the location of the earthquake using arrival times. Its magnitude is calculated with the frequency content of the P wave arrival (T_p) and the peak displacement (Pd) [15]. In the next stage, ground shaking is estimated using attenuation relations. As time passes, the data continues to flow. In this way, hazard maps are updated. Hazard assessments are revised in line with detailed ground-shaking observations from regions close to the epicenter. EPIC consists of three modules.

EPIC determines the location of an earthquake by detecting the P-waves generated after an earthquake by at least four stations. A grid search method is used for this determination. This method minimizes the difference between the calculated and observed arrival times [14]. The warning time can be defined as the time required to onset strong ground shaking. The earthquake's origin time and location information can be estimated using S-wave arrival time curves. Estimated values for S-wave arrival times need to be considered to determine the warning time conservatively [14].

The magnitude, a measure of the energy generated at the hypocenter during an earthquake, is estimated using the frequency characteristics of the first four seconds of the P wave. The vertical component waveform predominant period (τ_p) is calculated by the method proposed by Nakamura [16]. Various researchers have stated that the maximum predominant period ($T_p^{\max}$) in four seconds is scaled with the earthquake's magnitude [14,17-20]. To calculate τ_p, accelerometer records need to be converted to velocity records. Then, τ_p is continuously calculated in real-time with the equation (2.1).

$$\tau_i^p = 2\pi\sqrt{X_i/D_i} \tag{2.1}$$

Here, X_i and D_i in (2.1) can be written as follows:

$$X_i = \alpha X_{i-1} + x_i^2 \tag{2.2}$$

$$D_i = \alpha D_{i-1} + \left({dx}/{dt}\right)_i^2 \tag{2.3}$$

In (2.2), x_i represents the ground motion at the time i and α represents the 1-second smoothing constant (α=0.99 for 100 sps data, while α=0.95 for 20 sps data). x_i; velocity of the most recent data, X_i; is the square of the smoothed velocity. D_i used in (2.3); is the smoothed velocity data derivative (acceleration) square. The magnitude determination is faster since the frequency content of smaller magnitude events can be measured in a short time compared to large magnitude events. This also indicates that the magnitude estimation may increase as the duration of the data increases [14].

Allen and Kanamori [17] proposed two linear relations between the magnitude and $T_p^{\max}$ of events. For earthquakes ranging in magnitude from 3.0 to 5.0, a low-pass filter at 10 Hz is used. Magnitude estimation can be made when 1 second of data is used, but the error of estimate made with 2 seconds is slightly reduced. So additional data doesn't make the estimation any better. Then, by observing the $T_p^{\max}$ data (2.4) for magnitude estimation is determined (for magnitudes between 3.0 and 5.0). For earthquakes larger than 4.5, the best magnitude estimates can be obtained using a 3 Hz low-pass filter and 4-second data. The best-fit magnitude relationship for large earthquakes is given in (2.5) [14].

$$m_l = 6.3\log\left(\tau_p^{\max}\right) + 7.1 \tag{2.4}$$

$$m_h = 7.0\log\left(\tau_p^{\max}\right) + 5.9 \tag{2.5}$$

The relations are given for m_l and m_h are used by ElarmS to estimate the best-fit magnitude. The magnitude estimation process works like this: When a station is triggered 1 second after the event, m_l is estimated using

$\tau_p^{\max}$. When the data arrives in 2 seconds, the estimate is updated. The magnitude estimate of the event is determined by averaging the magnitudes estimated from each station. If the event magnitude is larger than 4.0, it is estimated in m_h. In this case, the magnitude is the average of the m_l and m_h estimated from all the triggered stations. The relationship between $T_p^{\max}$ and magnitude was tested using data of various magnitudes (3.0 to 8.3) from Southern California, Japan, and worldwide. Datasets from Southern California and Japan show similar scaling relations. The dataset from different countries for the Denali earthquake indicates that the scaling relation does not deteriorate even for the largest earthquakes [17-20].

The final step in the ElarmS process is to convert the location and magnitude estimate of the event into peak ground shaking prediction for all locations. Thus, ground shaking maps are obtained by mapping the spatial distribution of the peak ground shaking. Most current attenuation relations use only ground motion observations for earthquakes greater than 5.0, while ElarmS uses self-generated attenuation relations for earthquakes greater than 3.0. For continuous testing of Elarms, it is preferred to work on all earthquakes, small and large. The process of using ElarmS's attenuation relations is two steps. The magnitude estimation is made one second after the arrival of the first P wave. The estimated PGA from the empirical relations is calculated using this magnitude as a distance function.

As an event progresses, the stations closest to the epicenter begin to measure their PGAs. This information obtained is used to adapt the initial attenuation relations. The most essential function of the PGA observations is to remove the scatter of the predicted PGA. Allen [14] addressed different events and pointed out the inconsistency between the observations and estimates of attenuation relationships. He explained this as the most important reason that attenuation relationships do not consider the near-surface amplification effects. However, if known, these effects can be easily incorporated into ElarmS.

The new version of Elarms (E3) includes improvements to accurately predict damaging earthquakes, classify S-wave or teleseismic signals, and minimize the number of false alarms [15]. This latest version uses an experimental amplitude-period threshold to detect P-waves generated after a seismic event in California. Optimization will be necessary if, unlike California, this version of the algorithm is to be used in regions where the soil layer is not deep, such as the Korean Peninsula [16-19].

2.2. PRESTo

Probabilistic Earthquake Early Warning System (PRESTo) is an early warning system that integrates state-of-the-art algorithms to rapidly locate, estimate magnitude, and assess damage in real time. The algorithm is free and open source for all users. PRESTo can easily be used by a seismic network, by companies and scientists interested in early warning. The system is being used in real time in Italy, and real time tests are being carried out in some countries (South Korea, Romania, Türkiye). PRESTo processes real-time acceleration or velocity data to determine P-wave arrivals after an earthquake. These data are received from the stations via a SeisComP server and can also read data in SAC format for play back of the past data. When an earthquake occurs, whether real-time or simulated, the system immediately detects the event and generates shaking maps and location and magnitude estimates for the relevant regions. In the PRESTo algorithm, the earthquake location is obtained by a real-time probabilistic approach. Magnitude estimation is based on the peak displacement (Pd) in the first 2-4 seconds of the P waves using magnitude scaling relations. In subsequent operations, the ground motion is estimated with the prediction equations derived for this process [13]. Figure 2 shows a real interface image of PRESTo after replaying the Irpinia earthquake in 1980.

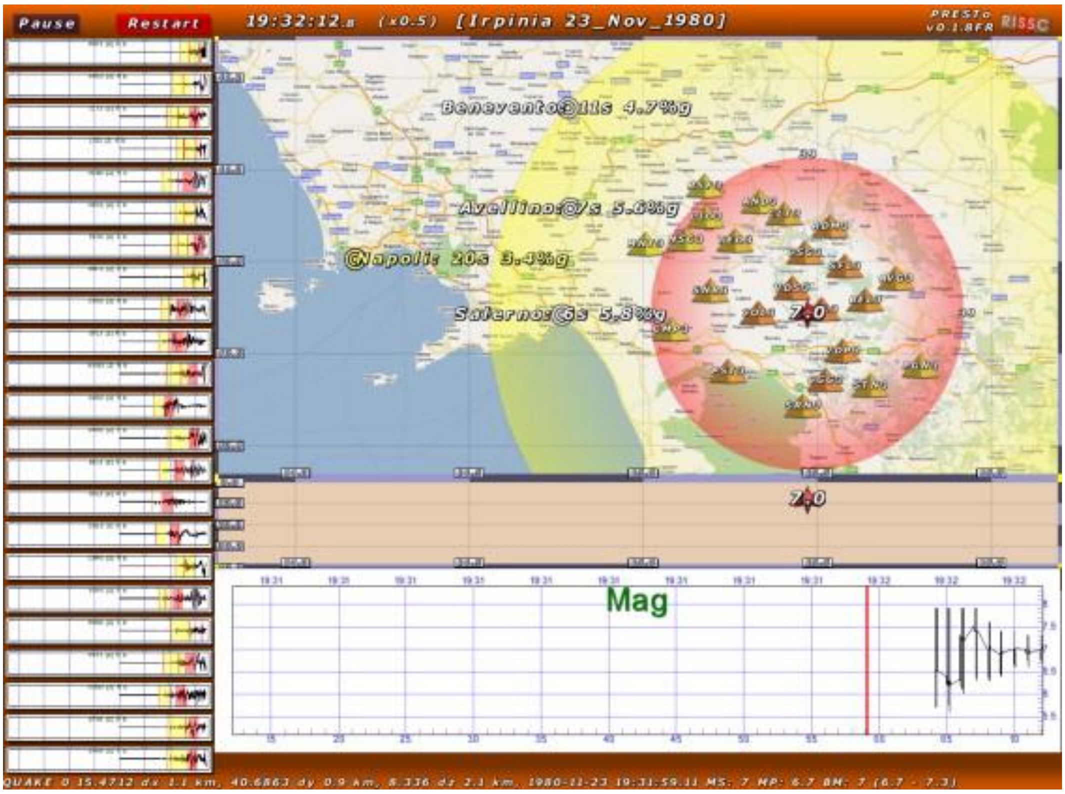

Figure 2. A real interface image of PRESTo after playback of synthetic traces for the 1980 Irpinia earthquake [13]

2.3. Virtual Seismologist (VS)

The Virtual Seismologist (VS) algorithm is based on the Bayesian approach and estimates an earthquake's magnitude, location, and ground shaking map using envelope attenuation relationships [21]. The Bayesian approach can be briefly defined as calculating a probability value using another known probability value. The location and magnitude parameters after an earthquake are estimated using ground motion ratios and attenuation relations within approximately three seconds after the first P-wave detected at the stations. The most important feature that distinguishes this method from others is the use of prior information. Preliminary information is especially useful in initial source estimates where limited data cannot obtain solutions. This preliminary information can be listed as the quality of the seismic network, the region's seismicity, the location of existing faults, and Gutenberg-Richter relations. The earlier earthquake forecasts can be made, the healthier early warnings can operate.

VS was developed, tested, and routinely run for the first time in Switzerland in 2013 for use within Seiscomp3 (SC3). It was then tested in six seismic networks worldwide (Greece, New Zealand, Romania, Türkiye, Iceland, and Southern California). SC3's widespread distribution and ease of installation made this wide application possible. Network operators already running SC3 for routine earthquake monitoring can incorporate VS(SC3) into their SC3 installation by updating to a version that includes VS(SC3) modules. The configuration of VS(SC3) modules is also detailed in the standard documentation of SC3.

Figure 3 shows the VS(SC3) processing flow. The arrows in the figure indicate the direction of the information flow represented by colors according to the sender type. The mediator (scmaster) and the orange modules are the heart of VS(SC3). The standard SC3 modules are used for P-wave detection (scautopick) and position detection (scautoloc). Scenvelope is a VS-specific preprocessing module. It provides a 1-s envelope data stream for all data (displacement, velocity, acceleration) and can access waves transmitted from different sources. Station and other information about the event can be kept in a meta-information. The scvsmag module of VS(SC3) performs a real-time magnitude calculation after an earthquake, which is continuously updated. Scvsmaglog is an EEW module and provides real-time warnings. These warnings can be taken by UserDisplay and Earthquake Early Warning Display (EEWD). Scolv is a graphical user interface that allows access to the entire database and records waveforms. It provides the possibility to analyze and review interactively [22,23].

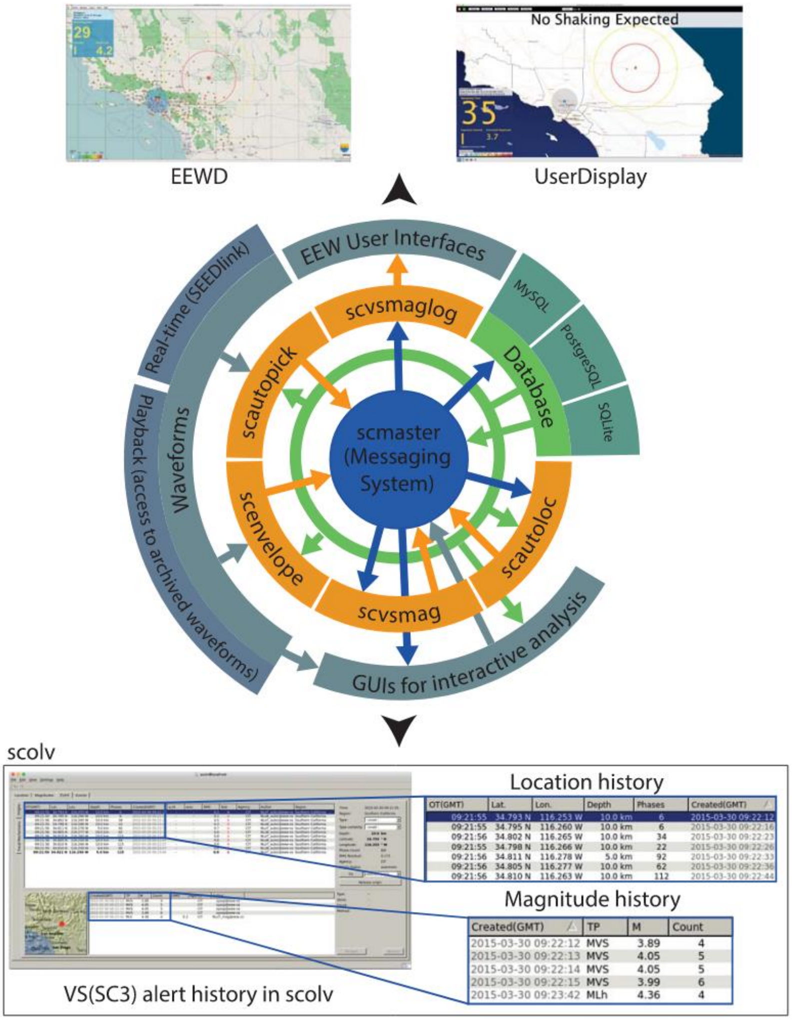

Figure 3. VS(SC3) processing flow [22]

2.4. UrEDAS/Compact UrEDAS

UrEDAS, Urgent Earthquake Detection and Alarm System, UrEDAS (Urgent Earthquake Detection and Alarm System) is the first representative of on-site early warning and the first operationalized system in the world [16]. The initial purpose of its application was to maintain the fast Japanese Railway Systems. In principle, UrEDAS uses the first three seconds of P waves as a basis for estimating parameters. First, the predominant period is used for magnitude estimation. Then the magnitude and P-wave amplitude allow the estimation of the epicentral distance. Particle motion is used to estimate the azimuth and depth of the earthquake. One of the advantages of UrEDAS is that all these processes are achieved with high accuracy with a single station [24].

Figure 4 (a) illustrates how only a single station defines the azimuth and P-wave. The figure also includes seismic wave recognition and the method of determining the epicenter-dependent azimuth with the three components of a single station. If the vertical component is larger than the horizontal component, it is defined as a P wave. The comparison between the back azimuths determined by UrEDAS and JMA is given in Figure 4 (b). The deviation of the back azimuths estimated by UrEDAS and JMA is approximately ±0.5. There is a relationship between the magnitudes of earthquakes and the lengths of ruptured faults. It is known that the larger the ruptured fault, the larger the earthquake. In addition, the earthquake's magnitude is also related to the duration and dominant period of the event. In this context, the earthquake's magnitude can be estimated by analyzing the dominant period of the initial motion (Figure 5).

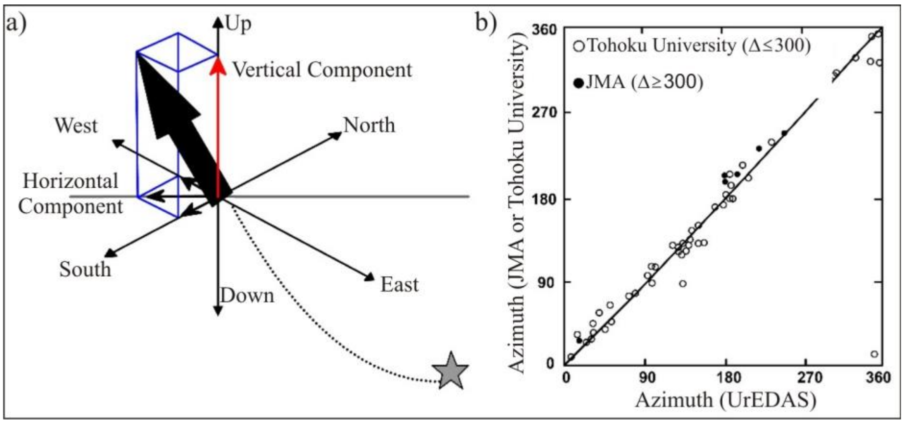

Figure 4. P-wave detection and back azimuth estimation [24]

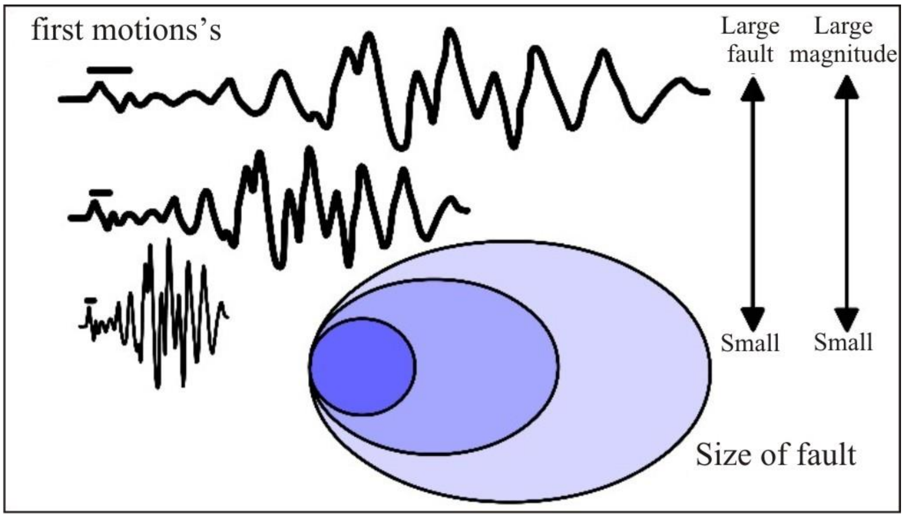

Figure 5. Relationship between first motion period and magnitude [24]

Unlike UrEDAS, Compact UrEDAS estimates the possible devastation after the earthquake directly from the earthquake motion and provides a warning if deemed necessary. UrEDAS performs this process with earthquake related parameters. The inner product of the acceleration and velocity vector obtains the hazard of the earthquake. This is called the destructive intensity (DI). However, the value obtained after this process is quite large. Therefore, the logarithm of the absolute value of the result is taken. DI value increases when the P wave is detected. It is recommended to use the PI value for the P wave alarm. PI is the largest DI value t time after detecting the P wave. Until the detection of the S-wave, the DI increases slowly and reaches its maximum value. This resulting value is associated with earthquake damage. This value is similar to the modified Mercalli intensity (MMI) or JMA instrumental intensity scale. DI has the advantage that it can be quickly determined in real-time after the P-wave is detected. Therefore, DI can be continuously monitored to provide a post-earthquake alert and estimate potential damage.

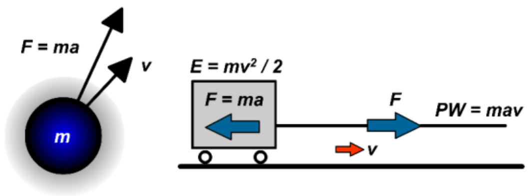

Figure 6. Relationship between acceleration, velocity, and intensity [24]

Based on Figure 6, the relationships between acceleration (cm/s2), velocity (cm/s), and intensity are given in (2.6)-(2.9). Here, *DI* is defined as Destructive Intensity, *RI* as Real-time Intensity, and *MMI* as Modified Mercalli Intensity.

$$PW = F \cdot v = m \cdot a \cdot v \tag{2.6}$$

$$DI = \log_{10}(a \cdot v) \tag{2.7}$$

$$RI = DI + 2.4 \tag{2.8}$$

$$MMI = (11/7) \cdot RI + 0.5 \tag{2.9}$$

The Compact UrEDAS uses similar operating principles to the UrEDAS. However, Compact UrEDAS provides faster alerts. It uses only a short period, such as one second of the P wave.

2.5. Real-time Earthquake Damage Reduction Precautions (ShakeAlert)

ShakeAlert was developed for the west coast of the United States in collaboration with the United States Geological Survey (USGS) and partners [25]. The system detects the P wave and estimates the earthquake's epicenter and magnitude. Then, by predicting the places expected to experience varying degrees of ground shaking, the ShakeAlert Message is issued [26,27]. This provides a warning before the S wave arrives, which produces strong shaking that causes damage. Accuracy and warning time are maximized as a combination of single stations and regional seismic network data is used. The warning period varies between 4 and 20 seconds depending on the fault type, the earthquake's focal depth, and the station's density close to the epicenter [28, 29]. The system has limitations: false and missed warnings are possible, and areas very close to the earthquake's epicenter may receive little or no warning. ShakeMap, a USGS Earthquake Hazards Program product, displays the intensity distribution automatically calculated from observed ground motion and is typically distributed to users a few minutes to 1 hour after an earthquake [30,31].

2.6. Next Generation Early Warning System

The capability of an EEWS is proportional to its ability to provide highly reliable real-time magnitude and shaking estimation in a short time. These parameters are also dependent on the accuracy of the source location. Therefore, improving the estimation of the earthquake location in EEWSs is very important. In the traditional systems, four or more stations need to be triggered for earthquake localization. Realizing this with fewer triggering stations is a challenge to overcome. Next-generation EEWSs are designed to improve the performance of location algorithms by utilizing real-time back azimuth. The next generation EEWS is roughly a real-time array-based location algorithm that gives an initial location estimate after S-wave arrival at the first array or after P-wave arrival at a second array [32]. If the location is calculated from only one array (if the arrays are in the same direction as the earthquake and the distance between the arrays is large), the location can be calculated when the S wave arrives after the first P wave before the P wave arrives in the second array. In other words, P-wave arrival to at least two arrays is required to calculate the location, or P and S-wave arrival to only one array is enough.

In the next generation of EEWS, the principles of array seismology are applied for real-time location determination. This system has two main modules: a single standalone array and multiple arrays. Waveform slowness and back azimuth are continuously monitored in a single standalone array. P and S wave arrivals are determined, and the back azimuth estimates distance and position. The resulting back azimuth determines the angle of the earthquake's location. This process is repeated with the second array. The closest distance at the intersection of the back azimuths of these two arrays is considered the earthquake's possible location. This estimated location information is updated when the next single station and array receive a P wave. Multiple arrays integrate data from several standalone modules. As P-wave arrivals occur, it collects multiple estimates of the back azimuth (BAZ) with surfaces of equal differential time (EDT). The real-time array method is advantageous for environments with sparse networks or unfavorable source-station configurations. The flowcharts of a single standalone array and multiple array modules are given in Figure 7 [32].

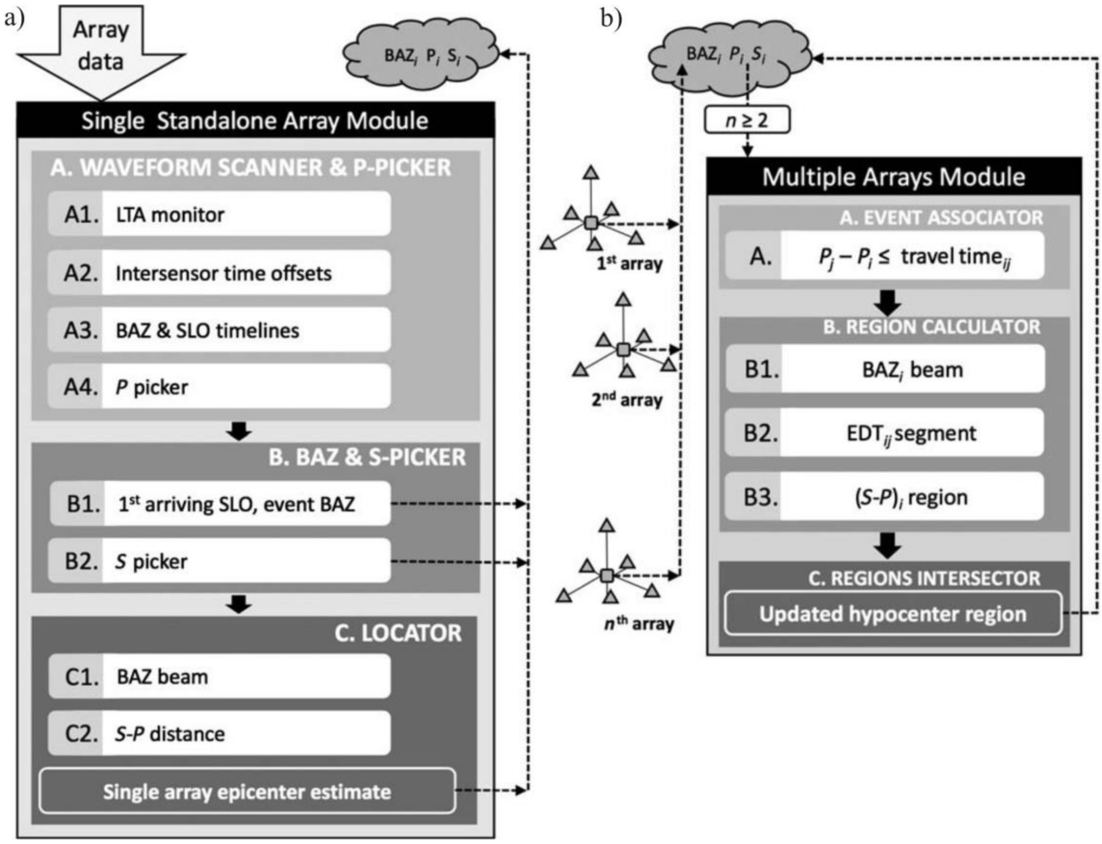

Figure 7. Flowcharts of a single standalone array (a) and multiple array modules. LTA stands for long-time average, and SLO stands for slowness [32]

Next generation EEWSs have significant advantages over the traditional EEWS. These advantages are low cost of network configuration, linear seismic network with omnidirectional sensing capability, use of artificial intelligence technology which eliminates false warnings, fast installation and quick implementation of the system, and reduction of P phase detection to less than 1 s. Figure 8 shows the interface of the next-generation early warning system. Next-generation EEWSs ideally consist of at least three stations in an array. These arrays can be triangular, quadrilateral, or diamond-shaped. It is important to know the location of each station. The distance between two arrays should be twice the distance of the fault to the array. Thus, if the fault is 10 km away, the distance between the two arrays should be 20 km.

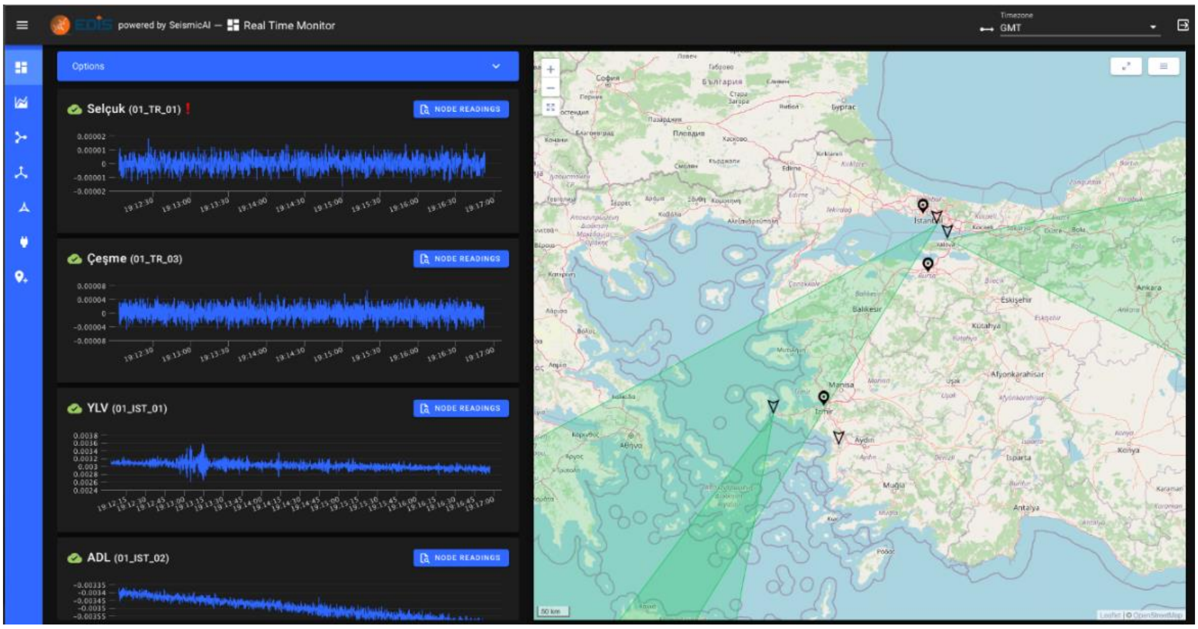

Figure 8. Next-generation early warning system user interface

2.6.1. An Earthquake Example for the Next Generation EEWS

On 26 September 2019 at 16.59 (GMT), an earthquake with ML= 5.7 occurred at about 13 km in the Marmara Sea (offshore Silivri). Very close to the epicenter of this earthquake, another earthquake with a magnitude of ML=3.5 occurred on 11 October 2023. This example uses the latest version of the seismic network around the Sea of Marmara, and its outputs are discussed.

The next generation early warning system first identifies the hypocenter region rapidly as the stations detect the P wave phase for the earthquake with ML=5.7. In the ML=5.7 earthquake in 2019, the small-aperture arrays were far from the epicenter because they had been installed a short time ago, and therefore the benefit could not be seen. In 2019, when the earthquake occurred, only one array was installed at the Kandilli Observatory of Boğaziçi University. The array was very far from the epicenter of the earthquake. Actually, the system was in the testing phase. The system did not provide positive results due to the necessity of detecting the S-wave in single arrays. The earthquake's epicenter can be reliably determined as the standard network consisting of a single station detects the P-wave phase (Figure 9) [33].

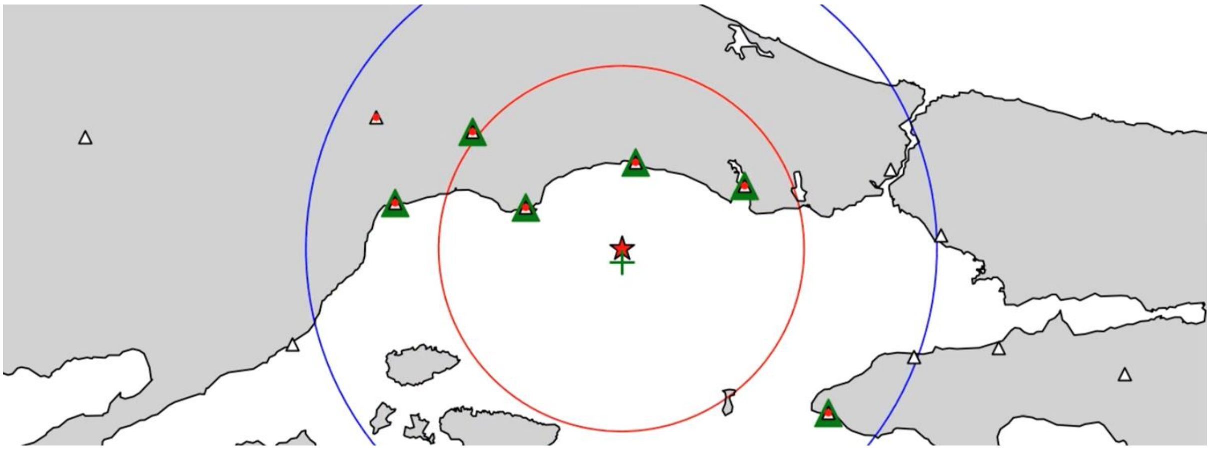

Figure 9. Determination of the epicenter location of the 26 September 2019 earthquake (ML=5.7) by the next generation EEWS. The red star represents the catalog location, green plus represents the location determined by the EEWS. The blue circle indicates the P wave, and the red circle indicates the S wave. Each triangle in the figure represents a single station. The green triangles and red-filled stations were used in the solution, and the P-wave was triggered

In the ML=3.5 earthquake on 11 October 2023, the network design with more frequent and better station distribution geometry than the earthquake in 2019 was used due to the network update made on the north coast before the earthquake (Figure 10). Figure 10 (a) shows the ML=5.7 earthquake analyzed in the standard single-station seismic network, and Figure 10 (b) shows the ML=3.5 earthquake analyzed in the hybrid network (both single station and array). In the traditional EEWS, a good station azimuthal distribution is needed to determine the magnitude and location of the earthquake. In the traditional EEWS, although two stations have P-wave triggers, a station's response in the south is expected to determine the magnitude and location (Figure 10 (a)). The solution starts when the P-wave arrives at the southern station. However, it is impossible to warn with the traditional EEW since the S wave will have already arrived at the settlements in the north by this time. As seen in Figure 10 (a), there is no solution when a P wave arrives at two of the traditional EEW stations. However, in the next generation EEWS, since there is an array at the locations of these stations, the first solution is provided with a 15 km error. In traditional EEW, it took 16 s to calculate the location and magnitude of the earthquake (due to high latencies). In the next generation EEWS, this time is 4 s. This is due to both low latencies and the use of different algorithms. The interface of the next generation EEWS, where an earthquake is analyzed, is shown in Figure 11.

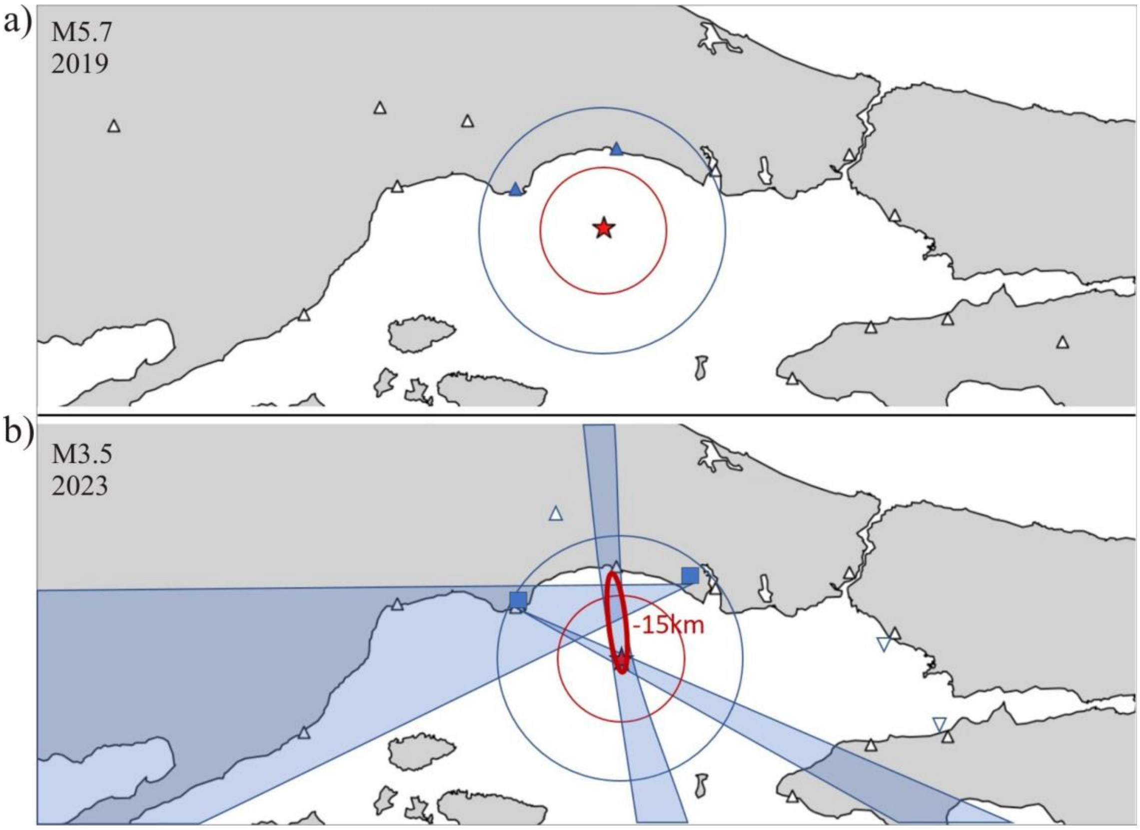

Figure 10. Earthquake epicenter determination with traditional (a) and next generation (b) EEWS. The top figure represents the 26 September 2019 earthquake (ML=5.7), and the bottom figure represents the 11 October 2023 earthquake (ML=3.5). The intersection of the back azimuths calculates the red ellipse in Figure 10 (b). Squares are arrays, and triangles are single stations. The symbols filled with blue are picked

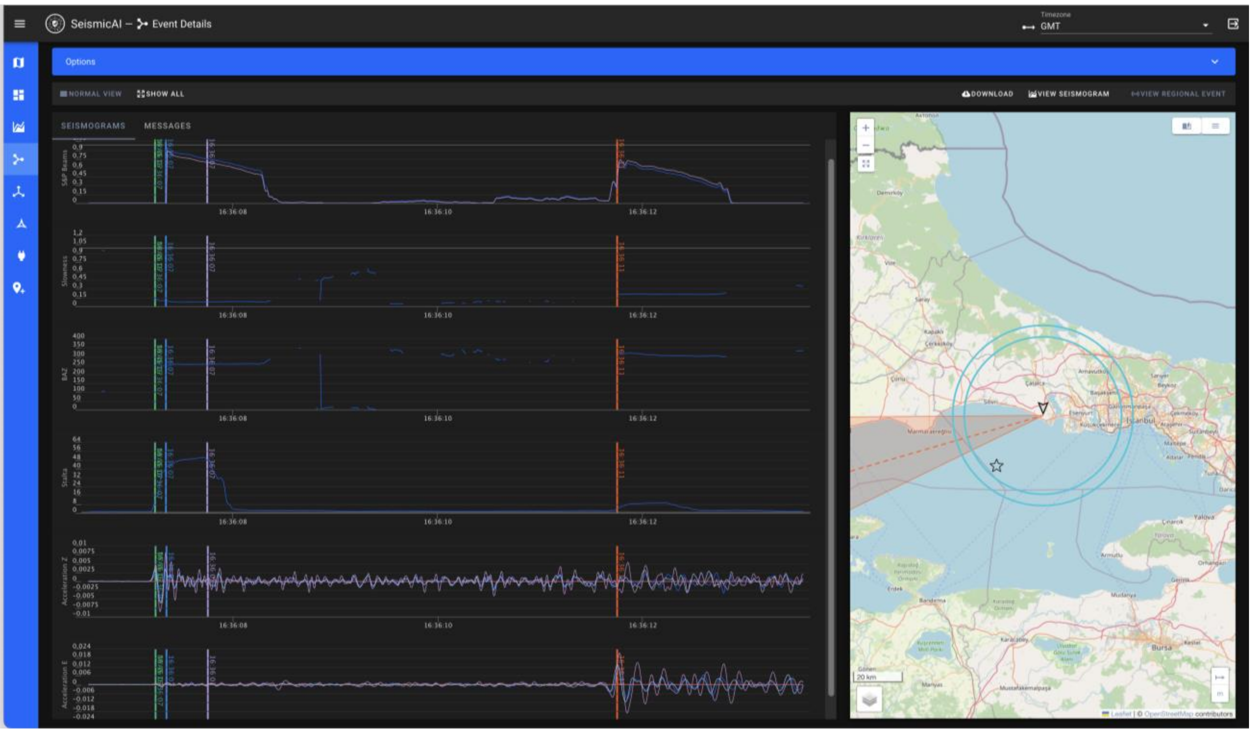

Figure 11. An example earthquake solution in a next-generation early warning interface. The black window on the left shows the event's slowness, back azimuth, P and S wave arrival times. The map on the right shows the back azimuth of the station and the possible location of the earthquake between the two blue circles

3. Conclusion

EEWS are systems that detect the onset of an earthquake and send timely warnings to the public or institutions. EEWS is an important tool in reducing loss of life, structural damage and economic losses. In the study, traditional and next-generation early warning algorithms are compared. The traditional EEW systems are widely used for regional warnings but have limitations such as the dependence of seismic warnings on the epicenter of the event, the same warning for every location, and false alarms or missed warnings. Next-generation EEW systems offer significant improvements to these limitations. The next-generation earthquake early warning algorithm has advantages such as low cost, detecting of earthquakes from anywhere, utilizing artificial intelligence algorithm for false warnings, fast installation and immediate operation of the system, and detecting P waves in a short time under 1 s. These advantages of next-generation early warning systems can provide an effective warning before potentially damaging earthquakes and eliminate the weaknesses of traditional warning systems.

Traditional EEWSs are particularly disadvantaged when faults with the potential to produce destructive earthquakes are located close to urban centers. The destructive S-wave can cause major destruction in densely populated areas until a warning is given. The best example of this can be an earthquake that may occur in the Marmara Sea. Next-generation EEWSs can overcome this weakness. Array-based location methodology quickly determines the epicenter, assesses the event's magnitude, estimates the ground shaking intensity, and issues a warning. It is a great advantage that the next generation EEWSs provide effective and fast solutions in regions like Türkiye, where very large earthquakes have occurred in the past. For this reason, further strengthening the next generation of EEWSs with the development of technology gains great importance in preventing all the losses that earthquakes will produce. The next generation of Earthquake Early Warning Systems (EEWS) can be used on a regional scale and in individual applications. While these systems are typically deployed across larger regions to provide widespread alerts, they are also adaptable in specific locations like factories, schools, homes, and other critical infrastructures.

Author Contributions

All the authors equally contributed to this work. They all read and approved the final version of the paper.

Conflicts of Interest

All the authors declare no conflict of interest.

Ethical Review and Approval

No approval from the Board of Ethics is required.

Acknowledgment

The preliminary findings of this study were presented at the 6th International Conference on Earthquake Engineering and Seismology held in Gebze, Türkiye, October 13-15, 2021. The authors would like to thank Andreas S. Eisermann for contributing to the study.

References

[1] S. Tunç, B. Tunç, D. Çaka, Ş. Barış, *Dünyada yaygın olarak kullanılan erken uyarı sistemleri*, 6th International Conference on Earthquake Engineering and Seismology, Kocaeli, 2021, pp. 895–909.

[2] R. N. Nof, R. M. Allen, *Implementing the ElarmS earthquake early warning algorithm on the Israeli seismic network,* Bulletin of the Seismological Society of America 106 (5) (2016) 2332–2344.

[3] G. Festa, M. Picozzi, A. Caruso, S. Colombelli, M. Cattaneo, L. Chiaraluce, L. Elia, C. Martino, S. Marzorati, M. Supino, A. Zollo, *Performance of earthquake early warning systems during the 2016–2017 Mw 5–6.5 Central Italy sequence*, Seismological Research Letters 89 (1) (2018) 1–12.

[4] Y. M. Wu, H. Mittal, T. C. Huang, B. M. Yang, J. C. Jan, S. K. Chen, *Performance of a low-cost earthquake early warning system (P-Alert) and shake map production during the 2018 Mw 6.4 Hualien, Taiwan, earthquake,* Seismological Research Letters 90 (1) (2019) 19–29.

[5] J. Santos-Reyes, *How useful are earthquake early warnings? The case of the 2017 earthquakes in Mexico City,* International Journal of Disaster Risk Reduction 40 (2019) 101148 11 pages.

[6] Y. Kodera, N. Hayashimoto, K. Moriwaki, K. Noguchi, J. Saito, J. Akutagawa, S. Adachi, M. Morimoto, K. Okamoto, S. Honda, M. Hoshiba, *First-year performance of a nationwide earthquake early warning system using a wavefield-based ground-motion prediction algorithm in Japan,* Seismological Research Letters 91 (2A) (2020) 826–834.

[7] A. I. Chung, M. A. Meier, J. Andrews, M. Böse, B. W. Crowell, J. J. McGuire, D. E. Smith, *ShakeAlert earthquake early warning system performance during the 2019 Ridgecrest earthquake sequence,* Bulletin of the Seismological Society of America 110 (4) (2020) 1904–1923.

[8] C. Peng, P. Jiang, Q. Ma, P. Wu, J. Su, Y. Zheng, J. Yang, *Performance evaluation of an earthquake early warning system in the 2019–2020 M 6.0 Changning, Sichuan, China, Seismic Sequence,* Frontiers in Earth Science 9 (2021) 699941 13 pages.

[9] S. Cho, J. K. Ahn, E. H. Hwang, *Optimization of network-based earthquake early warning systems on the Korean Peninsula*, IEEE Access 10 (2022) 83931–83939.

[10] M. Medina, R. Sanchez, S. Riquelme, M. C. Flores, P. Koch, F. Bravo, S. Barrientos, I. Henson, A. Chung, D. Melgar, C. Mpodozis, M. Hellweg, R. Allen, *An earthquake early warning system for Northern Chile based on ElarmS-3*, Seismological Society of America 93 (6) (2022) 3337–3347.

[11] S. Tunç, B. Tunç, E. Budakoğlu, D. Çaka, R. N. Nof, Ş. Barış, *Implementation of the EPIC earthquake early warning system in the Bursa Province (Türkiye) and its surroundings,* Applied Sciences 13 (8) (2023) 4985 17 pages.

[12] G. Cremen, C. Galasso, *Earthquake early warning: Recent advances and perspectives,* Earth-Science Reviews 205 (2020) 103184 15 pages.

[13] C. Satriano, L. Elia, C. Martino, M. Lancieri, A. Zollo, G. Iannaccone, *PRESTo, the earthquake early warning system for southern Italy: Concepts, capabilities and future perspectives*, Soil Dynamics and Earthquake Engineering 31 (2) (2011) 137–153.

[14] R. M. Allen, *The ElarmS earthquake early warning methodology and application across California, in earthquake early warning systems*, Springer, Berlin Heidelberg, 2007, Ch. 3, pp. 21–43.

[15] R. M. Allen, P. Gasparini, O. Kamigaichi, M Bose, *The status of earthquake early warning around the world: An introductory overview,* Seismological Research Letters 80 (5) (2009) 682–693.

[16] Y. Nakamura, *On the urgent earthquake detection and alarm system (UrEDAS),* in: Proceedings of Ninth World Conference on Earthquake Engineering, Tokyo, 1988, pp. 673–678.

[17] R. M. Allen, H. Kanamori, *The potential for earthquake early warning in southern California,* Science 300 (5620) (2003) 786–789.

[18] A. B. Lockman, R. M. Allen, *Single-station earthquake characterization for early warning*, Bulletin of the Seismological Society of America 95 (6) (2005) 2029–2039.

[19] E. L. Olson, R. M. Allen, *The deterministic nature of earthquake rupture,* Nature 438 (7065) (2005) 212–215.

[20] A. B. Lockman, R. M. Allen, *Magnitude-period scaling relations for Japan and the Pacific Northwest: Implications for earthquake early warning*, Bulletin of the Seismological Society of America 97 (1B) (2007) 140–150.

[21] G. Cua, T. Heaton, *The Virtual Seismologist (VS) method: A Bayesian approach to earthquake early warning*, in: P. Gasparini, G. Manfredi, J. Zschau (Eds.), Earthquake Early Warning Systems, Springer Berlin Heidelberg, Berlin, 2007, Ch. 7, pp. 97–132

[22] Y. Behr, J. F. Clinton, C. Cauzzi, E. Hauksson, K. Jónsdóttir, C. G. Marius, A. Pinar, J. Salichon, E. Sokos, *The Virtual Seismologist in SeisComP3: A new implementation strategy for earthquake early warning algorithms*, Seismological Research Letters 87 (2A) (2016) 363–373.

[23] F. Massin, J. Clinton, M. Böse, *Status of earthquake early warning in Switzerland*, Frontiers in Earth Science 9 (2021) 707654 20 pages.

[24] J. Saita, Y. Nakamura, *UrEDAS: The early warning system for mitigation of disasters caused by earthquakes and tsunamis*, in: J. Zschau, A. Küppers (Eds.), Early Warning Systems for Natural Disaster Reduction, Springer, Berlin, 2003, pp. 453–460.

[25] M. D. Kohler, E. S. Cochran, D. Given, S. Guiwits, D. Neuhauser, I. Hensen, R. Hartog, P. Bodin, V. Kress, S. Thompson, C. Felizardo, J. Brody, R. Bhada, S. Schwarz, *Earthquake early warning ShakeAlert system—West coast wide production prototype*, Seismological Research Letters 89 (1) (2018) 99–107.

[26] D. D. Given, S. E. Cochran, T. Heaton, E. Hauksson, R. Allen, P. Hellweg, J. Vidale, P. Bodin, *Technical implementation plan for the ShakeAlert production system— An earthquake early warning system for the West Coast of the United States*, U.S. Geological Survey Open-File Report (2014) 1097 25 pages.

[27] A. I. Chung, C. J. Neighbors, A. Belmonte, M. Miller, H. H. Sepulveda, C. Christensen, R. Jakka, E. S. Cochran, J. F. Lawrence, *The quake-catcher network rapid aftershock mobilization program following the 2010 M8.8 Maule, Chile earthquake*, Seismological Research Letters 82 (2011) 526–532.

[28] E. S. Cochran, B. T. Aagaard, R. M. Allen, J. Andrews, A. S. Baltay, A. J. Barbour, P. Bodin, B. A. Brooks, A. Chung, B. W. Crowell, D. D. Given, T. C. Hanks, J. R. Hartog, E. Hauksson, T. H. Heaton, S. McBride, M-A. Meier, D. Melgar, s. E. Minson, J. R. Murray, J. A. Strauss, D. Toomey, *Research to improve ShakeAlert earthquake early warning products and their utility*, U. S. Geological Survey Open-File Report (2018) 1131 17 pages.

[29] J. J. McGuire, D. E. Smith, A. D. Frankel, E. A. Wirth, S. K. McBride, R. M. de Groot, *Expected warning times from the ShakeAlert earthquake early warning system for earthquakes in the Pacific Northwest (ver. 1.1, March 24, 2021)*, U.S. Geological Survey Open-File Report (2021) 1026 37 pages.

[30] D. J. Wald, B. C. Worden, V. Quitoriano, K. L. Pankow, *ShakeMap manual: Technical manual, users guide, and software guide*, 12 (2005) A1.

[31] C. B. Worden, D. J. Wald, T. I. Allen, K. Lin, D. Garcia, G. Cua, *A revised ground-motion and intensity interpolation scheme for ShakeMap*, Bulletin of the Seismological Society of America 100 (6) (2010) 3083–3096.

[32] A. S. Eisermann, A. Ziv, H. G. Wust-Bloch, *Array-based earthquake location for regional earthquake early warning: Case studies from the Dead Sea transform*, Bulletin of the Seismological Society of America 108 (4) (2018) 2046–2053.

[33] A. S. Eisermann, *Hybrid small-aperture-array networks in EEW*, in: 5th International Conference on Earthquake Early Warning, İstanbul, 2023, pp. 16.